

# Nonlinear light behaviors near phase transition in non-parity-time-symmetric complex waveguides

Sean Nixon and Jianke Yang

*Department of Mathematics and Statistics, University of Vermont, Burlington, VT 05401, USA*

Many classes of non-parity-time ( $\mathcal{PT}$ ) symmetric waveguides with arbitrary gain and loss distributions still possess all-real linear spectrum or exhibit phase transition. In this article, nonlinear light behaviors in these complex waveguides are probed analytically near a phase transition. Using multi-scale perturbation methods, a nonlinear ordinary differential equation (ODE) is derived for the light's amplitude evolution. This ODE predicts that the first class of these non- $\mathcal{PT}$ -symmetric waveguides support continuous families of solitons and robust amplitude-oscillating solutions both above and below phase transition, in close analogy with  $\mathcal{PT}$ -symmetric systems. For the other classes of waveguides, the light's intensity always amplifies under the effect of nonlinearity even if the waveguide is below phase transition. These analytical predictions are confirmed by direct computations of the full system.

The study of complex optical potentials which still possess an all-real spectrum has its roots in parity-time ( $\mathcal{PT}$ ) symmetry. First introduced as a non-Hermitian generalization of quantum mechanics [1], this concept later spread to optics, where an even refractive index profile together with an odd gain and loss landscape constitutes a  $\mathcal{PT}$ -symmetric system [2]. In this optical setting,  $\mathcal{PT}$  symmetry has been experimentally realized [3–5]. A distinctive feature of  $\mathcal{PT}$ -symmetric systems is phase transition, where the spectrum turns from all-real to partially-complex when the gain-loss component (relative to the real refractive index) rises above a certain threshold [1–6]. This phase transition has been utilized in a number of emerging applications of  $\mathcal{PT}$ optics [7–9]. The added effects of nonlinearity into  $\mathcal{PT}$ -symmetric systems induce further novel properties which are being actively explored [10–18].

The downside of  $\mathcal{PT}$ optics lies in its restrictive construction, where the refractive index must be even while the gain and loss profile must be odd. Relaxing this restriction, non- $\mathcal{PT}$ -symmetric complex potentials with all-real spectra have been introduced [19–22]. In particular, many classes of non- $\mathcal{PT}$ -symmetric complex potentials with arbitrary gain-loss distributions and all-real spectra were reported in [22]. By tuning the free parameters in those complex potentials, phase transition could also be induced. In the linear regime, light in those different classes of non- $\mathcal{PT}$ -symmetric potentials behaves similarly [22]. In the presence of nonlinearity, will light still behave similarly in those different classes of potentials?

In this article, we analytically probe nonlinear light behaviors in these different classes of non- $\mathcal{PT}$ -symmetric complex potentials with all-real spectra and phase transition. Our analysis is focused near a phase transition, where a pair of real eigenvalues of the waveguide coalesce and form an exceptional point. Using multi-scale perturbation methods, a nonlinear ordinary differential equation (ODE) is derived for the light's amplitude evolution. This ODE predicts that the first class of these non- $\mathcal{PT}$ -symmetric waveguides support continuous fami-

lies of solitons and robust amplitude-oscillating solutions both above and below phase transition, closely resembling  $\mathcal{PT}$ -symmetric systems. For the other classes of waveguides, the light's intensity always amplifies under the effect of nonlinearity (even if the waveguide is below phase transition). These analytical results show that different classes of non- $\mathcal{PT}$ -symmetric waveguides exhibit different nonlinear behaviors.

The paraxial model for the propagation of light down a waveguide with a longitudinally uniform refractive index distribution and gain-loss landscape is the potential nonlinear Schrödinger (NLS) equation

$$i\Psi_z + \Psi_{xx} + V(x)\Psi + \sigma|\Psi|^2\Psi = 0, \quad (1)$$

where  $V(x)$  is a complex potential whose real part represents the linear refractive index and whose imaginary part represents gain and loss. If this potential satisfies the symmetry relation

$$\eta L = L^\dagger \eta, \quad (2)$$

where  $L = \partial_{xx} + V(x)$ ,  $\dagger$  represents the adjoint of an operator, and  $\eta$  is a Hermitian operator (i.e.,  $\eta^\dagger = \eta$ ), then when  $\eta$  has an empty kernel, the eigenvalues of  $L$  come in complex-conjugate pairs [22]. In that case, the spectrum of  $L$  is either all-real, or partially complex with conjugate pairs of eigenvalues. As an example, the class of  $\mathcal{PT}$ -symmetric potentials, where  $V^*(x) = V(-x)$ , falls within this framework when  $\eta$  is chosen as the parity operator,  $\mathcal{P}f(x) \equiv f(-x)$ . Here,  $*$  represents complex conjugation.

However, when  $\eta$  is chosen as a differential operator, wide classes of non- $\mathcal{PT}$ -symmetric potentials with all-real spectra can be obtained [22]. One such class of potentials, which we denote as Type-I, are

$$V(x; \gamma) = g^2(x) - 2\gamma g(x) + ig'(x), \quad (3)$$

where  $g(x)$  is an arbitrary real function, and  $\gamma$  is a free real parameter. For this type of potentials, the associated Hermitian operator  $\eta$  is

$$\eta(x; \gamma) = i\partial_x - g(x) + \gamma. \quad (4)$$

Another class of such potentials, which we denote as Type-II, are

$$V(x; \gamma) = \frac{1}{4}(g^2 - g_\infty^2) + \frac{g'^2 - 2gg''}{4g^2} + \gamma \left( \frac{1}{g^2} - \frac{1}{g_\infty^2} \right) + ig', \quad (5)$$

where  $g(x)$  is again an arbitrary real function,  $g_\infty = \lim_{x \rightarrow \pm\infty} g(x)$ , and  $\gamma$  is a free real parameter. Here we have assumed that  $g(x)$  approaches the same non-zero constant as  $x \rightarrow \pm\infty$  so that  $V(x)$  is localized.

In both types of potentials, since  $g(x)$  is arbitrary, the gain and loss profile (i.e., the imaginary part) of the potential can be arbitrary. Thus, these potentials are non- $\mathcal{PT}$ -symmetric in general. Yet, their spectra can still be all-real, which is surprising. Also notice that both potentials contain a free parameter ( $\gamma$ ). By tuning this parameter, phase transition can be induced [22].

To illustrate, we take

$$g(x) = \tanh 2(x+1) - \tanh(x-1) \quad (6)$$

in the Type-I potential (3), and

$$g(x) = \tanh 2(x+1) - \tanh(x-1) + 1 \quad (7)$$

in the Type-II potential (5). These two potentials are plotted in Fig. 1, for  $\gamma = 0.368$  and  $\gamma = 0.467$  respectively. They have the same gain-loss profile but different refractive index distributions. Both potentials are non- $\mathcal{PT}$ -symmetric; yet, their spectra are all-real (which we have verified numerically).

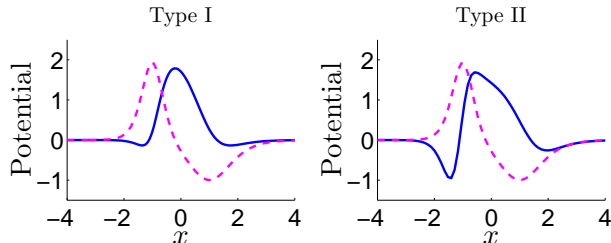


FIG. 1: (Left) Type-I potential with  $g(x)$  given by (6) and  $\gamma = 0.368$ . (Right) Type-II potential with  $g(x)$  given by (7) and  $\gamma = 0.467$ . Solid blue lines are  $\text{Re}(V)$  and dashed magenta  $\text{Im}(V)$ .

For the above  $g(x)$  functions, varying the parameter  $\gamma$  can induce a phase transition. For example, for Type-I potentials, the eigenvalue spectra for a range of  $\gamma$  values are displayed in Fig. 2 (top panel). Here, eigenvalues  $\mu$  are defined by  $L\psi = -\mu\psi$ . It is seen that at  $\gamma \approx 0.368$ , two discrete real eigenvalues collide, form an exceptional point, and then bifurcate off the real axis, thus a phase transition occurs. The Type-I potential displayed in Fig. 1 is at this phase-transition point.

Similarly, the tuning of  $\gamma$  can induce a phase transition in the Type-II potentials. This is shown in Fig. 2 (bottom panel), where a phase transition occurs at  $\gamma \approx 0.467$ . The potential at this point was displayed in Fig. 1 (right panel).

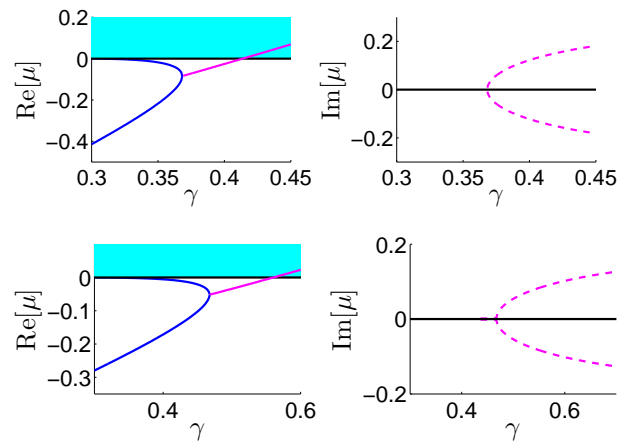


FIG. 2: Phase transitions in Type-I (top) and Type-II (bottom) potentials. Real eigenvalues are in solid blue, complex eigenvalues in magenta and the cyan region representing the continuous spectrum.

It is easy to notice from Fig. 2 that the spectra of Type-I and Type-II potentials behave quite similarly, which indicates that in the linear regime, solution dynamics in the two types of potentials would be largely similar. Then, in the nonlinear regime, would their solution dynamics still be similar? The answer is negative, as we will show analytically below.

For our analytical treatment, we focus on these potentials near a phase transition, where nonlinear solution dynamics can be determined by multi-scale perturbation methods. Suppose the spectrum of  $L$  has an exceptional point at  $\mu = \mu_0$  when  $\gamma = \gamma_0$  and consider the potentials nearby in the family, i.e.,  $\gamma = \gamma_0 + \epsilon$ , where  $|\epsilon| \ll 1$ . Then, up to order  $\epsilon$  the potential is

$$V(x; \gamma) \approx V_0(x) + \epsilon V_2(x),$$

where  $V_0(x) = V(x; \gamma_0)$  is the unperturbed potential at a phase transition, and  $V_2(x) = \frac{\partial}{\partial \gamma} V(x; \gamma)|_{\gamma=\gamma_0}$ . Defining

$$L_0 = \partial_{xx} + V_0(x) + \mu_0, \quad (8)$$

then since  $\mu_0$  is an exceptional point,  $L_0$  has one eigenfunction and at least one generalized eigenfunction where

$$L_0 u_e = 0, \quad L_0 u_g = u_e. \quad (9)$$

For simplicity, we assume the algebraic multiplicity of the exceptional point  $\mu_0$  is two, which is the generic case when two simple real eigenvalues coalesce (see Fig. 2). Then,  $L_0$  has a single generalized eigenfunction, i.e., the equation  $L_0 u_g = u_e$  does not admit a localized solution.

When the symmetry relation (2) is evaluated at  $\gamma = \gamma_0$ , we get  $\eta_0 L_0 = L_0^\dagger \eta_0$ , where  $\eta_0(x) = \eta(x; \gamma_0)$ . From this, we see that  $L_0^\dagger \eta_0 u_e = 0$ , i.e.,  $\eta_0 u_e$  is in the kernel of the adjoint operator  $L_0^\dagger$ . Thus, the solvability condition for the  $L_0 u_g = u_e$  equation is that

$$\langle u_e, \eta_0 u_e \rangle = 0, \quad (10)$$

where  $\langle f, g \rangle = \int_{-\infty}^{\infty} f g^* dx$  is the standard inner product. In addition, the non-solvability condition for the  $L_0 u_{g2} = u_g$  equation is that

$$D \equiv \langle u_g, \eta_0 u_e \rangle \neq 0. \quad (11)$$

Note that from  $L_0 u_e = 0$ , we have  $L_0^* u_e^* = 0$ . But for  $L_0$ ,  $L_0^\dagger = L_0^*$ , thus  $L_0^\dagger u_e^* = 0$ . Recalling  $L_0^\dagger \eta_0 u_e = 0$  above, we see that  $\eta_0 u_e = C u_e^*$ , where  $C$  is some constant.

Now we consider low-amplitude nonlinear solutions to Eq. (1) near this exceptional point. These solutions can be expanded into a multi-scale perturbation series,

$$\Psi(x, z) = \left( |\epsilon|^{\frac{1}{2}} u_1(x, Z) + |\epsilon| u_2 + |\epsilon|^{\frac{3}{2}} u_3 + \dots \right) e^{-i\mu_0 z},$$

where  $Z = |\epsilon|^{\frac{1}{2}} z$  is the slow-modulation scale. At the first three orders, we obtain the system of equations

$$\begin{aligned} L_0 u_1 &= 0, & L_0 u_2 &= -i u_{1Z}, \\ L_0 u_3 &= -i u_{2Z} - \rho V_2 u_1 - \sigma |u_1|^2 u_1, \end{aligned}$$

where  $\rho = \text{sgn}(\epsilon)$ . The  $u_1$  and  $u_2$  equations can be solved:

$$u_1 = A(Z) u_e(x), \quad u_2 = -i A'(Z) u_g(x).$$

Substituting them into the  $u_3$  equation, we get

$$L_0 u_3 = -A_{ZZ} u_g - A \rho V_2 u_e - \sigma |A|^2 A |u_e|^2 u_e,$$

whose solvability condition yields

$$A_{ZZ} - \alpha A + \sigma_1 |A|^2 A = 0, \quad (12)$$

where

$$\alpha = -\frac{\rho}{D} \langle V_2 u_e, \eta_0 u_e \rangle, \quad \sigma_1 = \frac{\sigma}{D} \langle |u_e|^2 u_e, \eta_0 u_e \rangle. \quad (13)$$

Eq. (12) is our reduced ODE model for nonlinear solution dynamics near an exceptional point in these non- $\mathcal{PT}$ -symmetric complex potentials.

Now we show that in this ODE model,  $\alpha$  is always real. In addition,  $\sigma_1$  is real for Type-I potentials but complex for other potentials such as Type-II.

First, we note that since  $L_0$  satisfies the symmetry relation  $\eta_0 L_0 = L_0^\dagger \eta_0$ , then

$$\begin{aligned} D^* &= \langle \eta_0 u_e, u_g \rangle = \langle \eta_0 L_0 u_g, u_g \rangle = \langle L_0^\dagger \eta_0 u_g, u_g \rangle \\ &= \langle \eta_0 u_g, L_0 u_g \rangle = \langle \eta_0 u_g, u_e \rangle = \langle u_g, \eta_0 u_e \rangle = D, \end{aligned}$$

thus  $D$  is real.

Next, we differentiate the symmetry equation (2) with respect to the free parameter  $\gamma$ , which yields  $\eta_{\gamma 0} L_0 + \eta_0 V_2 = V_2^* \eta_0 + L_0^\dagger \eta_{\gamma 0}$ , where  $\eta_{\gamma 0} = \frac{\partial}{\partial \gamma} \eta(x; \gamma)|_{\gamma=\gamma_0}$ . Then,

$$\begin{aligned} \langle V_2 u_e, \eta_0 u_e \rangle^* &= \langle \eta_0 u_e, V_2 u_e \rangle = \langle V_2^* \eta_0 u_e, u_e \rangle \\ &= \langle (\eta_0 V_2 + \eta_{\gamma 0} L_0 - L_0^\dagger \eta_{\gamma 0}) u_e, u_e \rangle \\ &= \langle \eta_0 V_2 u_e, u_e \rangle - \langle \eta_{\gamma 0} u_e, L_0 u_e \rangle = \langle V_2 u_e, \eta_0 u_e \rangle, \end{aligned}$$

thus,  $\alpha$  is real.

For the nonlinear coefficient  $\sigma_1$ , the symmetry relation alone is insufficient to guarantee a real constant. Instead, the form (4) of operator  $\eta$  associated with Type-I potentials must be employed. In this case,

$$\begin{aligned} \langle |u_e|^2 u_e, \eta_0 u_e \rangle &= \langle |u_e|^2 u_e, (i\partial_x - g + \gamma_0) u_e \rangle \\ &= \frac{1}{2} \text{Im} \langle u_e^2, (u_e^2)_x \rangle - \int_{-\infty}^{\infty} (g - \gamma_0) |u_e|^4 dx, \end{aligned}$$

thus,  $\sigma_1$  is real for Type-I potentials. However, for other types of potentials, it is generically complex as can be numerically verified.

The fact that  $\sigma_1$  is real for Type-I potentials but complex for other types of potentials has far-reaching consequences on the nonlinear dynamics in these potentials. When  $\sigma_1$  is real, the ODE (12) admits solutions with stationary amplitude,  $A(Z) = A_0 e^{-i\mu_1 Z}$ , where  $\mu_1$  is a free real parameter, and  $A_0$  is a constant given by

$$|A_0| = \sqrt{(\mu_1^2 + \alpha)/\sigma_1}. \quad (14)$$

This implies that under Type-I potentials, the full system (1) admits continuous families of solitons,  $\Psi(x; \mu) = u(x) e^{-i\mu z}$ , parameterized by  $\mu$ , where

$$\mu = \mu_0 + |\epsilon|^{\frac{1}{2}} \mu_1, \quad u(x) \approx |\epsilon|^{\frac{1}{2}} A_0 u_e(x).$$

In particular, when  $\alpha > 0$  (above phase transition) and  $\sigma_1 > 0$ , Eq. (14) predicts a soliton family above an amplitude threshold  $|A_0|_{min} = \sqrt{\alpha/\sigma_1}$ ; when  $\alpha < 0$  (below phase transition) and  $\sigma_1 < 0$ , Eq. (14) predicts a soliton family below an amplitude threshold  $|A_0|_{max} = \sqrt{\alpha/\sigma_1}$ . These predictions are verified in our numerics of the full system (1) (see also [21, 23, 24]).

However, when  $\sigma_1$  is complex, the ODE (12) does not admit solutions with stationary amplitude. This implies that under Type-II and higher-type potentials, the full system (1) does not admit continuous families of solitons. This is consistent with our direct numerics on this system, where soliton solutions could not be found.

Beyond solitons, the ODE (12) also predicts different behaviors on other types of solutions for real and complex  $\sigma_1$  values. If  $\sigma_1$  is real, Eq. (12) exhibits periodic orbits when  $\sigma_1 > 0$  (for either sign of  $\alpha$ ). This implies that under Type-I potentials, the full system (1) admits periodically-oscillating solutions under a suitable sign of nonlinearity both above and below phase transition. For example, for the Type-I potential with  $g(x)$  given by (6) and  $\epsilon = 0.05^2$  (above phase transition), a periodic orbit of the ODE under focusing nonlinearity ( $\sigma = 1$ ) is plotted in Fig. 3 (upper left panel). Numerically, we have found the corresponding solution in the PDE system (1), which is shown in the left panels of the same figure.

If  $\sigma_1$  is real, Eq. (12) also exhibits periodic orbits when  $\sigma_1 < 0$ ,  $\alpha < 0$ , and the initial amplitude is below a certain threshold (above this threshold, the ODE solution will blow up to infinity in finite distance). This

implies that under Type-I potentials, the full system (1) admits periodically-oscillating solutions (at low amplitude) and amplifying solutions (at high amplitude) under an opposite sign of nonlinearity below phase transition. As an example, we consider the same Type-I potential but with defocusing nonlinearity and  $\epsilon = -0.05^2$  (below phase transition). In this case, two ODE orbits, one periodic and the other amplifying, are plotted in Fig. 4 (upper left panel). These orbits match the corresponding solutions in the PDE system shown in the left panels of the same figure.

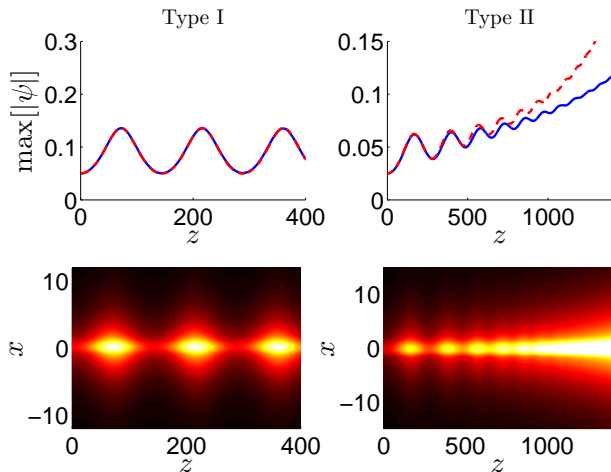


FIG. 3: Top: Comparisons of numerical simulations of the full system in solid blue against ODE results in dashed red for potentials above phase transition with focusing nonlinearity. Bottom: Solution evolutions in the full system. Left: Type-I potential. Right: Type-II potential.

However, if  $\sigma_1$  is complex, the ODE (12) does not admit periodic orbits. Instead, all solutions will amplify and blow up to infinity in finite distance. This implies that for other potentials such as Type-II, the PDE solutions will always amplify to high amplitude regardless of the sign of nonlinearity or whether the potential is above or below phase transition. To verify this behavior, we first consider an example Type-II potential with  $g(x)$  given by (7), where a phase transition occurs at  $\gamma_0 \approx 0.467$  and  $\mu_0 \approx -0.052$ . In this case, the coefficients in the ODE model are  $\alpha = \text{sgn}(\epsilon)0.093$  and  $\sigma_1 = \sigma(0.104 + i0.011)$ , where  $u_e(x)$  has been normalized to have unit peak amplitude. For  $\epsilon = 0.05^2$  (above phase transition) and  $\sigma = 1$  (focusing nonlinearity), an amplifying solution in the ODE model and the corresponding PDE solution are displayed in the right panels of Fig. 3, where good agreement can be seen. To verify the amplifying behavior below phase transition, we take this same Type-II potential but with  $\epsilon = -0.05^2$  and defocusing nonlinearity. In this case, an amplifying ODE solution and the corresponding PDE solution are displayed in the right panels of Fig. 4.

The above nonlinear dynamics in Type-I potentials is remarkably similar to that in  $\mathcal{PT}$ -symmetric potentials

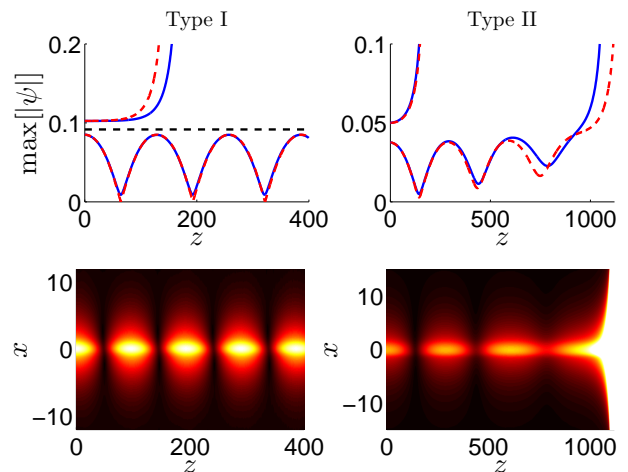


FIG. 4: Top: Comparisons of numerical simulations of the full system in solid blue against ODE results in dashed red for potentials below phase transition with defocusing nonlinearity. Bottom: Solution evolutions in the full system for the lower ODE orbits in the top panels.

[25]. In contrast, nonlinear dynamics in Type-II and higher-type potentials is quite different. Thus, we conclude that, even though all non- $\mathcal{PT}$ -symmetric potentials obeying the symmetry relation (2) for differential operators  $\eta$  exhibit similar linear behaviors, there is a large difference between Type-I potentials and the other potentials on nonlinear behaviors.

Why are Type-I potentials so special on nonlinear dynamics? One reason is that only for these potentials does the full system (1) admit a conservation law,

$$\frac{\partial}{\partial z} [\Psi(\eta\Psi)^*] + \frac{\partial J}{\partial x} = 0, \quad (15)$$

where  $\eta$  is given in Eq. (4), and the flux function  $J$  is

$$J = \Psi\Psi_{xx}^* - |\Psi_x|^2 + \frac{1}{2}\sigma|\Psi|^4 - i(g-\gamma)(\Psi\Psi_x^* - \Psi_x\Psi^*) - ig'|\Psi|^2.$$

The associated conserved quantity is  $I = \langle \Psi, \eta\Psi \rangle$ , where  $\frac{dI}{dz} = 0$ . For the other types of potentials, we could not find a conservation law. Apparently, this conservation law puts strong restrictions on the nonlinear dynamics in Type-I potentials.

In summary, nonlinear light behaviors in non- $\mathcal{PT}$ -symmetric complex waveguides obeying the symmetry condition (2) were probed analytically near a phase transition. It was found that nonlinear behaviors in Type-I waveguides are similar to those in  $\mathcal{PT}$ -symmetric systems, while those in other waveguides behave quite differently. Thus, these non- $\mathcal{PT}$ -symmetric waveguides exhibit a wider variety of nonlinear dynamics than  $\mathcal{PT}$ -symmetric waveguides.

This work was supported in part by Air Force Office of Scientific Research (USAF 9550-12-1-0244) and National Science Foundation (DMS-1311730).

- 
- [1] C.M. Bender and S. Boettcher, “Real spectra in non-Hermitian Hamiltonians having  $\mathcal{PT}$  symmetry”, *Phys. Rev. Lett.* **80**, 5243 (1998).
- [2] Z.H. Musslimani, K.G. Makris, R. El-Ganainy and D.N. Christodoulides, “Optical solitons in  $\mathcal{PT}$ -periodic potentials”, *Phys. Rev. Lett.* **100**, 030402 (2008).
- [3] C.E. Ruter, K.G. Makris, R. El-Ganainy, D.N. Christodoulides, M. Segev and D. Kip, “Observation of parity-time symmetry in optics”, *Nature Physics* **6**, 192 (2010).
- [4] A. Regensburger, C. Bersch, M.A. Miri, G. Onishchukov, D.N. Christodoulides and U. Peschel, “Parity-time synthetic photonic lattices”, *Nature* **488**, 167 (2012).
- [5] B. Peng, S. Özdemir, F. Lei, F. Monifi, M. Gianfreda, G. Long, S. Fan, F. Nori, C.M. Bender, and L. Yang, “Parity-time-symmetric whispering-gallery microcavities”, *Nat. Phys.* **10**, 394 (2014).
- [6] Z. Ahmed, “Real and complex discrete eigenvalues in an exactly solvable one-dimensional complex  $\mathcal{PT}$ -invariant potential”, *Phys. Lett. A* **282**, 343 (2001).
- [7] L. Feng, Y.L. Xu, W.S. Fegadolli, M.H. Lu, J.E.B. Oliveira, V.R. Almeida, Y.F. Chen, and A. Scherer, “Experimental demonstration of a unidirectional reflectionless parity-time metamaterial at optical frequencies”, *Nature Materials* **12**, 108 (2013).
- [8] L. Feng, Z.J. Wong, R. Ma, Y. Wang, and X. Zhang, “Single-mode laser by parity-time symmetry breaking”, *Science* **346**, 972 (2014).
- [9] H. Hodaei, M.A. Miri, M. Heinrich, D. N. Christodoulides, and M. Khajavikhan, “ $\mathcal{PT}$ -symmetric micro-ring laser”, *Science* **346**, 975 (2014).
- [10] R. Driben and B. A. Malomed, “Stability of solitons in parity-time-symmetric couplers”, *Opt. Lett.* **36**, 4323 (2011).
- [11] D. A. Zezyulin and V.V. Konotop, “Nonlinear modes in the harmonic  $\mathcal{PT}$ -symmetric potential”, *Phys. Rev. A* **85**, 043840 (2012).
- [12] S. Nixon, Y. Zhu and J. Yang, “Nonlinear dynamics of wave packets in  $\mathcal{PT}$ -symmetric optical lattices near the phase transition point”, *Opt. Lett.* **37**, 4874 (2012).
- [13] Y. Lumer, Y. Plotnik, M. C. Rechtsman, and M. Segev, “Nonlinearly induced  $\mathcal{PT}$  transition in photonic systems”, *Phys. Rev. Lett.* **111**, 263901 (2013).
- [14] U. Al Khawaja, S.M. Al-Marzoug, H. Bahlouli, and Y.S. Kivshar, “Unidirectional soliton flows in  $\mathcal{PT}$ -symmetric potentials”, *Phys. Rev. A* **88**, 023830 (2013).
- [15] Y.V. Kartashov, B.A. Malomed, and L. Torner, “Unbreakable  $\mathcal{PT}$  symmetry of solitons supported by inhomogeneous defocusing nonlinearity”, *Opt. Lett.* **39**, 5641 (2014).
- [16] M. Wimmer, A. Regensburger, M.A. Miri, C. Bersch, D.N. Christodoulides and U. Peschel, “Observation of optical solitons in  $\mathcal{PT}$ -symmetric lattices”, *Nature Communications* **6**, 7782 (2015).
- [17] S.V. Suchkov, A.A. Sukhorukov, J. Huang, S.V. Dmitriev, C. Lee and Y.S. Kivshar, “Nonlinear switching and solitons in  $\mathcal{PT}$ -symmetric photonic systems”, arXiv:1509.03378 (2015).
- [18] V.V. Konotop, J. Yang and D.A. Zezyulin, “Nonlinear waves in  $\mathcal{PT}$ -symmetric systems”, arXiv:1603.06826 (2016).
- [19] F. Cannata, G. Junker, and J. Trost, “Schrödinger operators with complex potential but real spectrum”, *Phys. Lett. A* **246**, 219 (1998).
- [20] M.A. Miri, M. Heinrich, and D. N. Christodoulides, “Supersymmetry-generated complex optical potentials with real spectra”, *Phys. Rev. A* **87**, 043819 (2013).
- [21] E.N. Tsoy, I.M. Allayarov and F. Kh. Abdullaev, “Stable localized modes in asymmetric waveguides with gain and loss”, *Opt. Lett.* **39**, 4215 (2014).
- [22] S. D. Nixon and J. Yang, “All-real spectra in optical systems with arbitrary gain and loss distributions”, *Phys. Rev. A* **93**, 031802(R) (2016).
- [23] V. V. Konotop and D. A. Zezyulin, “Families of stationary modes in complex potentials”, *Opt. Lett.* **39**, 5535 (2014).
- [24] S. D. Nixon and J. Yang, “Bifurcation of soliton families from linear modes in non- $\mathcal{PT}$ -symmetric complex potentials”, arXiv:1509.07057 (2015).
- [25] S. D. Nixon and J. Yang, “Nonlinear wave dynamics near phase transition in  $\mathcal{PT}$ -symmetric localized potentials”, arXiv:1506.04445 (2015).